Published in final edited form as:
Biomaterials. 2010 May ; 31(14): 3840–3847. doi:10.1016/j.biomaterials.2010.01.104.

Biomimetic hydrogels with pro-angiogenic properties

James J. Moon[*], **Jennifer E. Saik**[*], **Ross A. Poche**[†], **Julia E. Leslie-Barbick**[*], **Soo-Hong Lee**[*], **April A. Smith**[*], **Mary E. Dickinson**[†], and **Jennifer L. West**[*,‡]

[*]Department of Bioengineering, Rice University, P.O. Box 1892, MS 142, Houston, Texas 77251-1892

[†]Department of Molecular Physiology and Biophysics, Baylor College of Medicine, One Baylor Plaza BCM 335, Houston, Texas 77030

Abstract

To achieve the task of fabricating functional tissues, scaffold materials that can be sufficiently vascularized to mimic functionality and complexity of native tissues are yet to be developed. Here, we report development of synthetic, biomimetic hydrogels that allow the rapid formation of a stable and mature vascular network both *in vitro* and *in vivo*. Hydrogels were fabricated with integrin binding sites and protease-sensitive substrates to mimic the natural provisional extracellular matrices, and endothelial cells cultured in these hydrogels organized into stable, intricate network of capillary-like structures. The resulting structures were further stabilized by recruitment of mesenchymal progenitor cells that differentiated into smooth muscle cell lineage and deposited collagen IV and laminin *in vitro*. In addition, hydrogels transplanted into mouse cornea were infiltrated with host vasculature, resulting in extensive vascularization with functional blood vessels. These results indicate that these hydrogels may be useful for applications in basic biological research, tissue engineering, and regenerative medicine.

Introduction

Most successes in tissue engineering have been limited to thin or avascular tissues such as skin, bladder, and cartilage as these constructs are relatively simple in design without requirement for intricate blood vessels [1-4]. Although there have been recent advances in vascularization of tissue constructs *in vivo* [5], development of complex tissues or organs such as heart, kidney, liver and lung has been elusive due to lack of proper formation of vasculature in the engineered constructs. Thus, the most impending challenge in creating more complex and clinically relevant tissues is vascularization of engineered tissues.

The process of angiogenesis is achieved by complex interactions among endothelial cells (ECs), the interstitial extracellular matrix (ECM), and the neighboring mural cell types via various growth factors [6,7]. In the initial phase of angiogenesis, vascular endothelial growth factor (VEGF) activates ECs from their normal quiescent states. When activated, the ECs proliferate and secrete various proteases, including matrix metalloproteinases (MMPs), to degrade the basement membrane and ECM. ECs migrate through and extend sprouts to build tubular structures. These nascent vessels are stabilized by recruitment of mural cells such

‡To whom correspondence should be addressed. Dr. Jennifer L. West, Department of Bioengineering, Rice University, P.O. Box 1892, MS 142, Houston, TX 77251-1892. Phone: (713) 348-5955. Fax: (713) 348-5877. jwest@rice.edu.

mesenchymal stem cells (MSCs), which differentiate into pericytes and deposit new ECM proteins form basal lamina [8,9].

As these multi-components are all essential part of neovascularization, the design of pro-angiogenic tissue constructs need to address each component in order to truly mimic the physiological microenvironment in which ECs can form functional blood vessels. The objectives of the present study were to integrate cellular, biochemical, and biophysical cues in synthetic biomaterials to achieve extensive vascularization both *in vitro* and *in vivo*. To achieve this, hydrogels mimicking natural provisional ECM were synthesized and assessed as a scaffold for angiogenesis.

To fabricate synthetic ECM-mimicking biomaterials, we used protease-sensitive PEG hydrogels, first reported by West and Hubbell [10]. Protease-sensitive peptides were introduced into the backbone of PEG to render PEG-hydrogels biodegradable in response to cellular proteases. These types of materials can also be modified with cell adhesive sequences for use as scaffolds in regenerative medicine [11-16]. In the present study, we examined proteolytically-degradable and cell-adhesive PEG hydrogels as provisional matrices for angiogenesis both *in vitro* and *in vivo*. To form and stabilize new blood vessels in hydrogels, we exploited cellular interactions between ECs and MSCs; co-culture of ECs and MSCs in hydrogels led to formation of extensive tubule-like structures that were stabilized, not subject to regression, for long term culture *in vitro*. In addition, we demonstrate vascularization of these hydrogels with functional blood vessels *in vivo*.

Materials and Methods

Cell maintenance

Human umbilical vein endothelial cells (HUVECs) were obtained from Cambrex (East Rutherford, NJ). The cells were grown on endothelial cell medium EGM-2 (Cambrex) supplemented with 2 mM L-glutamine, 1000 U/mL penicillin, and 100 mg/L streptomycin (Sigma, St. Louis, MO), and they were used through passage 8. 10T1/2 cells (American Type Culture Collection, Rockville, MD) were grown and maintained in DMEM supplemented with 10% fetal bovine serum (FBS), 2 mM L-glutamine, 1000 U/mL penicillin, and 100 mg/L streptomycin, and they were used through passage 18. All cells were incubated at 37 °C in a 5% CO_2 environment.

Synthesis of PEG-polymer hydrogel precursors

A MMP-sensitive peptide sequence, GGGPQG↓IWGQGK was synthesized by solid phase peptide synthesis based on standard Fmoc chemistry using an Apex396 peptide synthesizer (Aapptec, Louisville, KY, USA). Hydrogels with this peptide in the polymer backbone have been shown to be completely degraded by matrix metalloproteinases (MMP) [11]. Following purification, synthesis of the peptide was confirmed with matrix-assisted laser desorption ionization time of flight mass spectrometry (MALDI-ToF; Bruker Daltonics, Billerica, MA, USA)

Synthesis of the ABA block copolymers with the peptide linker was completed as described previously [10]. Briefly, the MMP-sensitive peptide sequence was reacted with acrylate-PEG-*N*-hydroxysuccinimide (acrylate-PEG-NHS, 3400 Da; Nektar) in a 1:2 (peptide: PEG) molar ratio in 50 mM sodium bicarbonate buffer (pH 8.5) for 2 h. This step conjugates a PEG-monoacrylate chain to the N-terminus and to the amine group on the lysine at the C-terminus of the peptide. The resulting product was then dialyzed (MWCO 5,000; Spectrum Laboratories, Inc., Rancho Dominguez, CA, USA) to remove unreacted peptide and PEG moieties, and the product was lyophilized, frozen, and stored under argon at - 80 °C. The cell adhesive ligand,

Arg-Gly-Asp-Ser, (RGDS, American Peptide, Sunnyvale, CA) was conjugated to acrylate-PEG-NHS in 1:1 molar ratio under the similar conditions. Fluorophore-tagged PEG-RGDS was synthesized by reacting PEG-RGDS with Alexa Fluor-488 carboxylic acid (Invitrogen) in 10-fold dye molar excess in DMF. $VEGF1_{65}$ (Sigma) was conjugated to acrylate-PEG-SMC in 200:1 molar ratio at pH 8.5 at 4 °C for 4 days, followed by final 4 hours at 24 °C. The resulting PEG-VEGF solution was then lyophilized and reconstituted in HEPES buffered saline (HBS) with 0.1% BSA at 4°C until use. A gel permeation chromatography system equipped with UV-vis and evaporative light scattering detectors (Polymer Laboratories, Amherst, MA) was used to analyze the products.

Fabrication of MMP-sensitive PEG hydrogels

The hydrogel precursor solution was prepared in 10 mM HBS (pH 7.4) with PEG-RGDS (3.5 μmol/mL), a photoinitiator, Irgacure-2969 (0.3 mg/ml; Ciba Corporations, Basel, Switzerland), and varying amount of MMP-sensitive PEG-GGGPQGIWGQGK-PEG. In this work, MMP-sensitive PEG precursor was added to the final concentrations of 7.5 mg/ml, 10 mg/ml, 12.5 mg/ml, and 15 mg/ml to fabricate hydrogels with polymer weight percentages of 7.5%, 10%, 12.5%, and 15%, respectively. For HUVECs only culture, 6×10^6 cells were added to the hydrogel precursor solution. For HUVEC and 10T1/2 co-culture, 4.8×10^6 HUVECs and 1.2×10^6 10T1/2 cells were added. On coverglasses that had been cleaned with 70% ethanol and sterilized under UV lamp over night, the PEG precursor-cell suspension was dispensed as 5 μl droplets and photopolymerized by exposure to long-wavelength UV light (365 nm, 10 mW/cm^2) for 7 min. The hydrogels were then immersed with EGM-2 media and incubated at 37 °C in a humidified atmosphere containing 5% CO_2. For PEG hydrogels used in corneal angiogenesis assay *in vivo*, VEGF was mixed into the polymer solution to create concentrations of 512 ng VEGF per gel and 1.9 ng PEG-VEGF per gel.

Characterization of hydrogels

The swelling ratio and water content of the hydrogels were then determined as described previously [17]. The compressive moduli of the different hydrogels with and without cells were determined using a 10 N load cell at a crosshead speed of 0.5 mm/min in an Instron-3342 (Canton, MA) mechanical tester as previously described [18]. Degradation rates of MMP-sensitive PEG hydrogels formulated with varying polymer weight percentages were measured by monitoring the release of tryptophan (W) in the MMP-sensitive peptide sequence with a UV-Vis spectrophotometer (Carey 5000 Varian, Walnut Creek, CA) at 280 nm.

Measurement of tubule length and the number of branching points in 3D network of hydrogels

Endothelial tubule formation was evaluated by measuring total tubule length formed and the number of branching points over 6 days. On day 1, 3, and 6, cells in the hydrogels were stained with 2 μM calcein AM and visualized with a confocal microscopy (Zeiss LIVE 5, Carl Zeiss, Thornwood, NY) with z stack depth ranging 100-200 m. Scion Image (Scion Corporation, Frederick, MD) was used to trace and measure the total tubule length and the number of branching points in each area. The data were normalized to the z stack depth in each area to account for the different optical slice volumes of the images.

Time-lapse video confocal microscopy

To record time-lapse images during endothelial tubule formation, HUVECs and 10T1/2 were pre-labeled with 50 μg CellTracker Green CMFDA (5-chloromethylfluorescein diacetate; Invitrogen) and 50 μg CellTracker Red CMTPX (Invitrogen), respectively, per manufacturer's instructions prior to encapsulation in the hydrogels. After photoencapsulation of the cells, the hydrogels were incubated in EGM-2 media for 5 hrs before time-lapse imaging. A confocal

microscope (Zeiss LIVE 5) equipped with a motorized XYZ stage and a temperature hood was used to record time-lapse images. T he temperature hood was perfused with 5% CO_2 during the experiments. Confocal images were obtained at 1 hr intervals for 66 hrs, and the motorized stage allowed automatic collection of images from pre-recorded, multiple locations.

Isolation of cellular lysates and Western blotting

The hydrogels were prepared as 5 μl droplets each with either HUVEC monoculture (24×10^6 cells/ml), 10T1/2 mono-culture (6×10^6 cells/ml), or HUVECs and 10T1/2 co-culture (24×10^6 and 6×10^6 cells/ml, respectively). After 6 days, the cells were isolated from the bulk of hydrogels by degrading away the hydrogels with 2 mg/ml collagenase-1 solution (Sigma) for 10 min at 37 °C. Cell suspensions from four 5 μl hydrogel droplets were pooled for each cell culture condition to obtain enough cell lysate for Western blotting. In parallel experiments, cells were plated on 6 well tissue culture plates with either HUVEC mono-culture (24×10^4 cells/well), 10T1/2 mono-culture (6×10^4 cells/well), or HUVECs and 10T1/2 co-culture (24×10^4 and 6×10^4 cells/well, respectively). SDS-PAGE and Western blotting were performed following a stand protocol. The primary antibodies used for Western blotting include antibodies against smooth muscle α-actin (SM-αactin, 1:3000; ABCam, Cambridge, MA), calponin (1:500; ABCam), and caldesmon (1:500; Sigma). The secondary antibody was used at 1:2000, 1:1000, and 1:1000 dilutions, respectively.

Immunofluorescence staining

Immunofluorescence staining was performed to confirm differentiation of 10T1/2 cells into SMC lineages and to visualize deposition of ECM proteins adjacent to the tubular structures. On day 1 and 6, the hydrogels containing HUVEC and 10T1/2 co-culture were fixed, permeabilized, and stained with primary and secondary antibodies. The primary antibodies used were mouse anti-SMα-actin (Sigma), rabbit anti-CD31 (Bethyl), rabbit anti-collagen-type IV (ABCam), and rabbit anti-laminin (Sigma) IgGs. The secondary antibodies were anti-rabbit and anti-mouse antibodies conjugated with either Alexa flour 488, Alexa fluor 594, or rhodamine (Invitrogen). For some samples, actin cytoskeletons and nuclei were stained with TRITC-conjugated phalloidin (5 U/ml, Sigma) for 1 h and DAPI (300 nM, Invitrogen) for 5 min.

Hydrogel implantation into the mouse cornea

Using a modified version of the previously described corneal micropocket angiogenesis assay [19], hydrogels were implanted into mouse cornea in *Flk1-myr::mCherry* transgenic mouse, which exhibits EC-specific expression of a myristoylated mCherry fluorescence protein in EC membrane [20]. Briefly, mice were anesthetized, and a partial thickness incision was made into the mouse cornea. The micropocket was created using a von Graef knife, and hydrogels were implanted into the micropocket immediately after UV photopolymerization. Seven days post-implantation, some mice were injected intravenously with dextran-Texas red (MW 70KDa), and the mice were sacrificed with CO_2 asphyxiation. Eyes from the mice were enucleated and fixed in 4% paraformaldehyde for one hour at 4°C. Corneal flat-mount preparations were made, and imaging was performed using a Zeiss LSM 510 META inverted microscope system (Carl Zeiss Inc) equipped with a Zeiss Plan-Apochromat 20×/0.75 NA objective. 543-nm and 488-nm lasers were used to excite the *Flk1-myr::mCherry* and fluorophore-tagged PEG-RGDS, respectively.

Statistical Analysis

Statistical analysis was performed with Jmp 5.1 (SAS Institute Inc, Cary, NC). Data sets were analyzed using two-way analysis of variance (ANOVA), followed by Tukey's HSD test for

multiple comparisons. *P*-values less than 0.05 were considered statistically significant. All values are reported as mean ± standard deviation.

Results and Discussion

Proteolytically-degradable hydrogel and its mechanical characterization

To fabricate synthetic ECM-mimicking hydrogels used in the current studies, we incorporated an MMP-sensitive sequence (GGGPQG↓IWGQGK) into the backbone of PEG block polymers with acrylate terminal groups, which allow crosslinking of precursors into networks [10,11, 21] (Figure 1A). GGGPQG↓IWGQGK is a mutated version of α1(I) collagen chain for increased degradation kinetics with various MMPs [11,22]. In addition, a ligand for integrin, RGDS, was grafted onto PEG chains to support integrin-mediated cellular adhesion and migration while VEGF was incorporated into hydrogels to promote robust angiogenesis [12, 23].

We first characterized protease-mediated degradation of hydrogels. Degradation of the hydrogels was monitored by measuring release of tryptophan from the MMP-sensitive sequences in hydrogels incubated with collagenase, a subset of MMP family of proteases (Figure 1B). Hydrogels with 10% polymer weight percentage incubated with collagenase solution underwent complete degradation within 1.5 hrs, but not with either plasmin or the buffer solution even after 21 hrs, demonstrating specificity of degradation mediated by MMP family of proteases. Susceptibility of hydrogels to proteolysis was correlated with their polymer weight percentage as denser networks took progressively longer time to degrade (Figure 1C). As the polymer weight percentage was increased from 7.5% to 15%, the compressive modulus of the hydrogels was increased from 30.2 ± 6.05 kPa to 110 ± 23.8 kPa (Figure 1G). Encapsulation of cells did not alter the compressive moduli of hydrogels. The swelling ratios for the 7.5, 10, 12.5, and 15% hydrogels were 27.9 ± 8.37, 17.0 ± 2.59, 14.7 ± 3.11, and 13.2 ± 2.33, and their water contents were 96.2 ± 1.11, 94.0 ± 0.903, 92.9 ± 1.47, and 92.3 ± 1.28 %, respectively.

Co-culture of HUVECs and 10T1/2 cells in hydrogels for angiogenesis

To form and stabilize new blood vessels in hydrogels, we exploited heterotypic cell interactions between ECs and mesenchymal progenitor cells. ECs are able to form primitive tubule structures when cultured alone; however, for the rudimentary blood vessels to become matured and stabilized, they require interaction with mural cell types. 10T1/2 cells, a subset of multipotent mesenchymal progenitor cells, are known to support endothelial tubule formation in naturally occurring ECM-derived materials [24-26].

MMP-sensitive PEG hydrogel precursors were formulated with human umbilical vein endothelial cells (HUVECs) and 10T1/2 cells (30 million cell/ml with HUVEC:10T1/2 ratio of 4:1) and exposed to long wavelength UV to photopolymerize the precursors into hydrogels. The cells encapsulated in hydrogels were cultured, and examined for their angiogenic responses at various time points (Figure 1D, E, F). In order to find the optimal mechanical composition of the hydrogels for the angiogenic responses, tube formation by HUVECs and 10T1/2 cells were quantified in hydrogels with 7.5% to 15% polymer weight percentage. In hydrogels with an intermediate polymer weight percentage of 10%, HUVECs and 10T1/2 cells formed primitive tubule-like structures by day 3 and continued to mature into extensive interconnections throughout the 3D network of hydrogels over 6 days. In soft, compliant hydrogels with 7.5% polymer weight, the cells underwent self-assembly to form thick interconnections, but the resulting structures rapidly regressed as the gels were completely degraded within 6 days. In stiffer hydrogels with 12.5 or 15% polymer weight, the degree of tubule formation was reduced as cells failed to migrate as much in softer matrices, and the cell

clusters remained short and rudimentary. In contrast, HUVECs and 10T1/2 cells co-cultured on tissue culture plates for 14 days did not form any tubule-like structures but remained as monolayers. The varying degrees of angiogenic responses in these hydrogels did not seem to result from different cellular viability as more than 80% of cells remained viable after 6 days in all hydrogel formulations tested, which is within a typical range reported in other literatures using hydrogel systems (Supplement Figure 1) [27, 28]. These results show that angiogenesis organized and promoted by HUVECs and 10T1/2 cells are well recapitulated in proteolytically-degradable hydrogels and that there is a particular formulation of hydrogels with an intermediate rigidity that maximizes these angiogenic responses.

These results do not demonstrate mechanical properties of hydrogels as a sole determinant of angiogenic potential since other parameters such as density of cell adhesive ligand or degradable sites were not held constant. However, since 10% polymer weight PEG hydrogels produced robust angiogenic responses, all the subsequent studies were performed with this particular formulation of hydrogels unless noted otherwise.

Dynamics of tubule formation by HUVECs and 10T1/2 cells

To better understand the dynamics of angiogenesis in the hydrogels, the process of tubule formation was captured by time-lapse confocal microscopy. In hydrogels with HUVECs in mono-culture condition (30 million cells/ml), the cells started migrating toward each other to form large clusters (t = 5 hr) and organized into primitive tubule-like structures (t = 21 hr) (Figure 2A, C, and Supporting Video 1). However, at later time points (t = 53 and 69 hr), the structures lost their tubular morphology and rapidly regressed into individual cell clusters. The total tubule length decreased over 6 day culture period, while the number of branching points stayed at minimal levels (Supplementary Figure 2).

In contrast, HUVECs and 10T1/2 cells co-cultured in the hydrogels (30 million cell/ml with HUVEC:10T1/2 ratio of 4:1) formed large clusters that rapidly organized into tubule-like structures throughout the hydrogels (t = 21 and 37 hr) (Figure 2B, and Supporting Video 2). The tubule-like structures were maintained stably even at later time points (t = 53 and 69 hr) with extensive branches and typical length reaching 700 μm (Figure 2C, and Supplementary Figure 2).

The endothelial tubular structures formed were reminiscent of capillary structures in their cellular organizations and morphology. 10T1/2 cells were frequently observed to align adjacent to and migrate rapidly along the tubular structures that were assembled by HUVECs. Figure 2D shows HUVECs undergoing lumen formation and 10T1/2 cells adjacent to the ECs supporting the process. Subsets of the HUVECs had multiple small vesicles, while others had their vesicles fused together intercellularly to form lumens enclosed by multiple ECs (Figure 2D, E), and these processes of lumen formation and perivascular association of mural cell types parallel a series of physiological events that accompany neovascularization as described recently *in vivo* [29]. In addition, HUVECs and 10T1/2 cells kept in culture for 28 days maintained their extensive network of tubular structures throughout the hydrogels (Figure 2F), demonstrating their durability. The hydrogels remained intact and stable when examined up to 1 month. Taken together, these results suggest that 10T1/2 cells enhance endothelial tubule formation and maintenance in hydrogels.

Differentiation of 10T1/2 cells toward smooth muscle cell lineage

We next addressed the question whether 10T1/2 MSCs differentiate toward SMC lineages in co-culture conditions with HUVECs. 10T1/2 cells are known to up-regulate expressions of smooth muscle marker proteins, such as SM-myosin, SM22α, and calponin when co-cultured together with ECs [24]. We indeed observed dramatic up-regulation of SMC protein markers

such as SM α-actin, calponin, and caldesmon in the co-culture conditions in hydrogels, but not in mono-culture conditions of either cell type as examined by Western blotting (Figure 3A). Similar results were obtained from cells cultured in tissue culture plates. Over-proliferation of either cell type contributing to this result can be ruled out since time-lapse confocal images revealed a minimal number of cell division during 72 hrs of culture as reported in the literature [30].

Differentiation of 10T1/2 cells into SMC lineages was further confirmed by immunofluorescence staining. There was minimal level of SM α-actin staining on day 1 in the hydrogels with co-culture conditions, while anti-CD31 staining showed HUVECs dispersed in the matrix (Figure 3B). After 6 days, anti-CD31 staining showed HUVECs in tubule-like structures, whereas the cells stained with anti-SM α-actin antibody aligned adjacent to the HUVECs (Figure 3C). Taken together, these results suggest that 10T1/2 precursor cells differentiate toward SMC lineages in co-culture conditions and associate closely with the tubule-like structures composed of HUVECs.

Cellular remodeling of hydrogels

Collagen-type IV and laminin, both the major components of basal lamina of blood vessels [31,32], were found to be secreted and deposited along the tubule-like structures (Figure 3D-G). This indicates that these cells actively remodel the matrices by secreting their own set of ECM proteins, which are known to serve as reservoir for various growth factors and provides structural integrity to newly formed capillaries [33].

Formation of functional blood vessels *in vivo*

Proteolytically-degradable PEG hydrogels were implanted into mouse cornea using a micropocket angiogenesis assay [19] and examined 7 days post-implantation (Figure 5A,B). We utilized *Flk1-myr::mCherry* transgenic mice, which exhibit EC-specific expression of a reporter mCherry in EC membrane [20] and allow monitoring of host vasculature invading into the hydrogels by confocal microscopy. In order to recruit the host blood vessels into hydrogels, pro-angiogenic growth factor, VEGF, was incorporated into the hydrogels both in a soluble and an immobilized form via PEG linkage as described previously [23]. In the absence of VEGF, there was not any significant angiogenic response (Supplement Figure 3). VEGF released from non-degradable hydrogels lacking MMP-sensitive peptide sequence promoted neovascularization underneath, but not in the hydrogels as shown by the vessels in red in the depth profile graph (Figure 4A-D). In contrast, MMP-sensitive PEG hydrogels with 10% polymer weight had significant portions of the scaffold degraded after 7 days, and robust neovascularization was observed (Figure 4E-H). The newly formed vessels infiltrated into the core of hydrogels as shown in green in the depth profile graph (Figure 4H). Dextran-Texas red (MW 70KDa) was injected intravenously in the host mice to delineate functionality of the blood vessels formed in the hydrogels. Figure 5C shows that indeed the blood vessels in the hydrogels were functional and perfused with the host's circulatory system. More rigid hydrogels with 15% polymer weight showed the initial stages of vessel penetration into the hydrogels (Figure 4L arrow); however, cells failed to invade into the core of hydrogels (Figure 4I-L). These data in corroboration with the *in vitro* results indicate that degradation of hydrogels and the ensuing formation of functional blood vessels can be controlled by provision of appropriate biophysical and biochemical cues in the hydrogels.

Conclusions

This work aimed to combine cellular, biochemical, and biomechanical cues to promote neovascularization in synthetic biomaterials. By providing appropriate cellular and molecular components in microenvironment that mimics physiological landscape of angiogenesis, we

have been able to recapitulate and promote blood vessel formation both *in vitro* and *in vivo* in completely synthetic biomaterials. These results suggest applications of these systems for angiogenesis and anti-angiogenesis studies including its development as a diagnostic platform for screening angiogenic and anti-angiogenic compounds as well as clinical applications in tissue engineering and regenerative medicine.

Supplementary Material

Refer to Web version on PubMed Central for supplementary material.

Acknowledgments

This work was supported by grants from NIH and NSF. The authors would like to thank Iris Kim, Melissa Scott, and Tegy Vadakkan for technical support.

References

1. Langer R, Vacanti JP. Tissue engineering. Science 1993;260:920–926. [PubMed: 8493529]
2. Gentzkow GD, Iwasaki SD, Hershon KS, Mengel M, Prendergast JJ, Ricotta JJ, et al. Use of dermagraft, a cultured human dermis, to treat diabetic foot ulcers. Diabetes Care 1996;19:350–354. [PubMed: 8729158]
3. Atala A, Bauer SB, Soker S, Yoo JJ, Retik AB. Tissue-engineered autologous bladders for patients needing cystoplasty. Lancet 2006;367:1241–1246. [PubMed: 16631879]
4. Temenoff JS, Mikos AG. Review: tissue engineering for regeneration of articular cartilage. Biomaterials 2000;21:431–440. [PubMed: 10674807]
5. Levenberg S, Rouwkema J, Macdonald M, Garfein ES, Kohane DS, Darland DC, et al. Engineering vascularized skeletal muscle tissue. Nat Biotechnol 2005;23:879–884. [PubMed: 15965465]
6. Folkman J, DAmore PA. Blood vessel formation: What is its molecular basis? Cell 1996;87:1153–1155. [PubMed: 8980221]
7. Jain RK. Molecular regulation of vessel maturation. Nat Med 2003;9:685–693. [PubMed: 12778167]
8. Bell SE, Mavila A, Salazar R, Bayless KJ, Kanagala S, Maxwell SA, et al. Differential gene expression during capillary morphogenesis in 3D collagen matrices: regulated expression of genes involved in basement membrane matrix assembly, cell cycle progression, cellular differentiation and G-protein signaling. J Cell Sci 2001;114:2755–2773. [PubMed: 11683410]
9. Davis GE, Senger DR. Endothelial extracellular matrix: biosynthesis, remodeling, and functions during vascular morphogenesis and neovessel stabilization. Circ Res 2005;97:1093–1107. [PubMed: 16306453]
10. West JL, Hubbell JA. Polymeric biomaterials with degradation sites for proteases involved in cell migration. Macromolecules 1999;32:241–244.
11. Lutolf MP, Lauer-Fields JL, Schmoekel HG, Metters AT, Weber FE, Fields GB, et al. Synthetic matrix metalloproteinase-sensitive hydrogels for the conduction of tissue regeneration: engineering cell-invasion characteristics. Proc Natl Acad Sci U S A 2003;100:5413–5418. [PubMed: 12686696]
12. Zisch AH, Lutolf MP, Ehrbar M, Raeber GP, Rizzi SC, Davies N, et al. Cell-demanded release of VEGF from synthetic, biointeractive cell ingrowth matrices for vascularized tissue growth. FASEB J 2003;17:2260–2262. [PubMed: 14563693]
13. Mann BK, Gobin AS, Tsai AT, Schmedlen RH, West JL. Smooth muscle cell growth in photopolymerized hydrogels with cell adhesive and proteolytically degradable domains: synthetic ECM analogs for tissue engineering. Biomaterials 2001;22:3045–3051. [PubMed: 11575479]
14. Lee SH, Moon JJ, West JL. Three-dimensional micropatterning of bioactive hydrogels via two-photon laser scanning photolithography for guided 3D cell migration. Biomaterials 2008;29:2962–2968. [PubMed: 18433863]
15. Lutolf MP, Raeber GP, Zisch AH, Tirelli N, Hubbell JA. Cell-responsive synthetic hydrogels. Adv Mater 2003;15:888–892.

16. DeForest CA, Polizzotti BD, Anseth KS. Sequential click reactions for synthesizing and patterning three-dimensional cell microenvironments. Nat Mater 2009;8:659–664. [PubMed: 19543279]
17. Canal T, Peppas NA. Correlation between mesh size and equilibrium degree of swelling of polymeric networks. J Biomed Mater Res 1989;23:1183–1193. [PubMed: 2808463]
18. Bikram M, Fouletier-Dilling C, Hipp JA, Gannon F, Davis AR, Olmsted-Davis EA, et al. Endochondral bone formation from hydrogel carriers loaded with BMP2-transduced cells. Ann Biomed Eng 2007;35:796–807. [PubMed: 17340196]
19. Rogers MS, Birsner AE, D'Amato RJ. The mouse cornea micropocket angiogenesis assay. Nature protocols 2007;2:2545–2550.
20. Poche RA, Larina IV, Scott ML, Saik JE, West JL, Dickinson ME. The Flk1-myr::mCherry mouse as a useful reporter to characterize multiple aspects of ocular blood vessel development and disease. Dev Dyn 2009;238:2318–2326. [PubMed: 19253403]
21. Lee SH, Miller JS, Moon JJ, West JL. Proteolytically degradable hydrogels with a fluorogenic substrate for studies of cellular proteolytic activity and migration. Biotechnol Progr 2005;21:1736–1741.
22. Barrett, AJ.; Rawlings, ND.; Woessner, JJF. Handbook of Proteolytic Enzymes. San Diego: Academic Press; 1998.
23. Leslie-Barbick JE, Moon JJ, West JL. Covalently-Immobilized Vascular Endothelial Growth Factor Promotes Endothelial Cell Tubulogenesis in Poly(ethylene glycol) Diacrylate Hydrogels. J Biomat Sci 2009;20:1763–1779.
24. Hirschi KK, Rohovsky SA, D'Amore PA. PDGF, TGF-beta, and heterotypic cell-cell interactions mediate endothelial cell-induced recruitment of 10T1/2 cells and their differentiation to a smooth muscle fate. J Cell Biol 1998;141:805–814. [PubMed: 9566978]
25. Koike N, Fukumura D, Gralla O, Au P, Schechner JS, Jain RK. Creation of long-lasting blood vessels. Nature 2004;428:138–139. [PubMed: 15014486]
26. Wang ZZ, Au P, Chen T, Shao Y, Daheron LM, Bai H, et al. Endothelial cells derived from human embryonic stem cells form durable blood vessels in vivo. Nat Biotechnol 2007;25:317–318. [PubMed: 17322871]
27. Mahoney MJ, Anseth KS. Three-dimensional growth and function of neural tissue in degradable polyethylene glycol hydrogels. Biomaterials 2006;27:2265–2274. [PubMed: 16318872]
28. Williams CG, Malik AN, Kim TK, Manson PN, Elisseeff JH. Variable cytocompatibility of six cell lines with photoinitiators used for polymerizing hydrogels and cell encapsulation. Biomaterials 2005;26:1211–1218. [PubMed: 15475050]
29. Kamei M, Saunders WB, Bayless KJ, Dye L, Davis GE, Weinstein BM. Endothelial tubes assemble from intracellular vacuoles in vivo. Nature 2006;442:453–456. [PubMed: 16799567]
30. Hirschi KK, Rohovsky SA, Beck LH, Smith SR, D'Amore PA. Endothelial cells modulate the proliferation of mural cell precursors via platelet-derived growth factor-BB and heterotypic cell contact. Circ Res 1999;84:298–305. [PubMed: 10024303]
31. Schlingemann RO, Rietveld FJ, Kwaspen F, van de Kerkhof PC, de Waal RM, Ruiter DJ. Differential expression of markers for endothelial cells, pericytes, and basal lamina in the microvasculature of tumors and granulation tissue. Am J Pathol 1991;138:1335–1347. [PubMed: 1711288]
32. Beltramo E, Buttiglieri S, Pomero F, Allione A, D'Alu F, Ponte E, et al. A study of capillary pericyte viability on extracellular matrix produced by endothelial cells in high glucose. Diabetologia 2003;46:409–415. [PubMed: 12687340]
33. Mancuso MR, Davis R, Norberg SM, O'Brien S, Sennino B, Nakahara T, et al. Rapid vascular regrowth in tumors after reversal of VEGF inhibition. J Clin Invest 2006;116:2610–2621. [PubMed: 17016557]

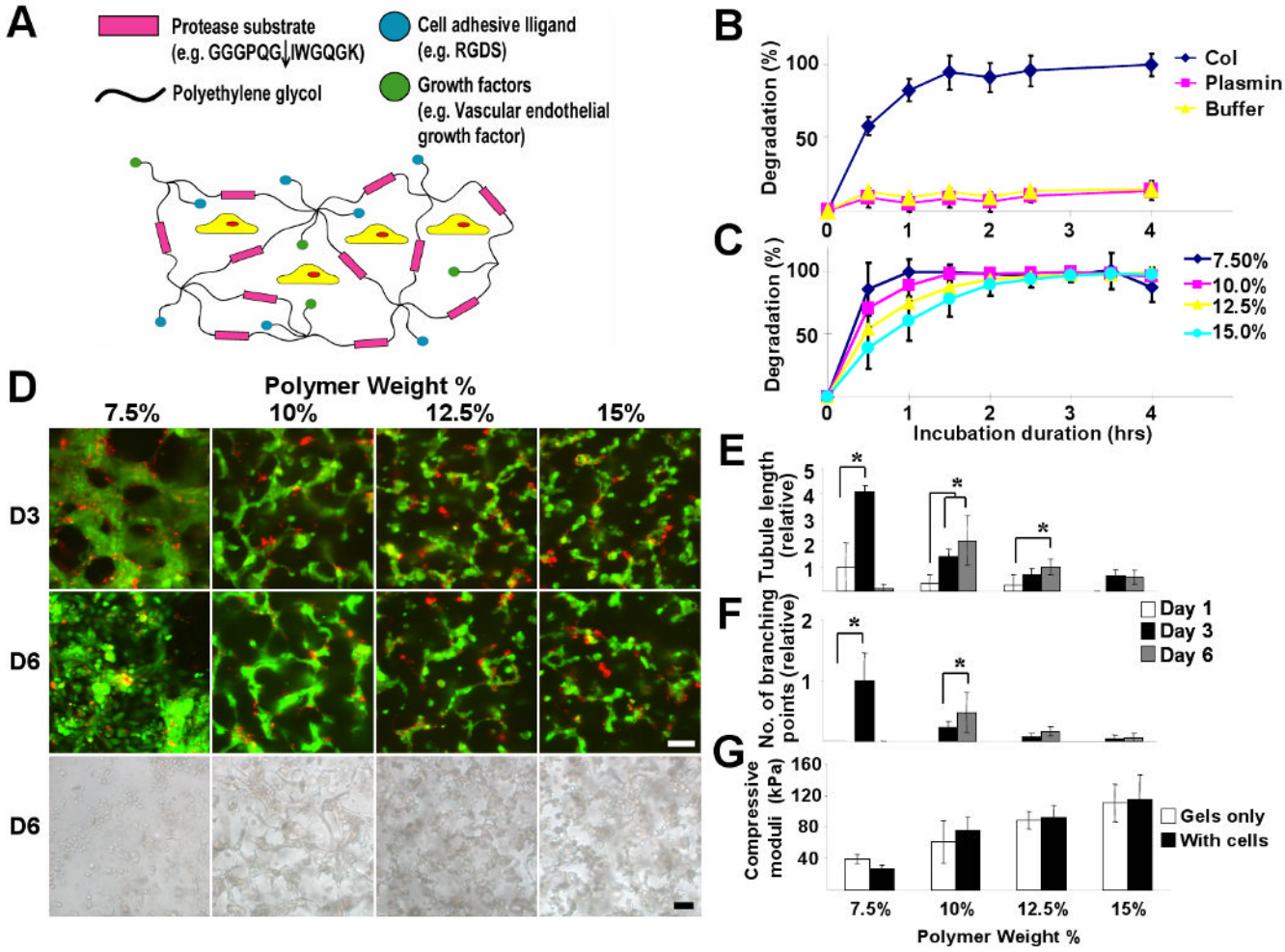

Figure 1. Proteolytically-degradable PEG hydrogels with intermediate rigidity support endothelial tubule formation and maintenance

A) The schematic illustration shows fabrication of MMP-sensitive PEG hydrogels by UV polymerization of PEG-RGDS and PEG chain with MMP-sensitive peptide in its backbone in the presence of cells. B) Hydrogels were degraded by collagenase (10 μg/ml), but not by plasmin (10 μg/ml) or buffer solutions. C) Hydrogels fabricated with different polymer weight percentages exhibited varying degradation profiles in collagenase (10 μg/ml) solution. D) Confocal and bright field images of HUVECs and 10T1/2 cells cultured for 3 and 6 days in hydrogels with varying polymer weight percentages. HUVECs and 10T1/2 cells were pre-stained with CytoTracker green and red, respectively, prior to encapsulation in hydrogels. E) The total tubule length formed and F) the number of branching point were measured during 6 day culture period in hydrogels formulated with varying polymer weight percentages. Only in hydrogels with intermediate polymer weight percentage (10%), HUVECs and 10T1/2 cells formed stable tubule-like structures. G) Compressive moduli ranging from 30 to 110 kPa were measured in hydrogels with and without encapsulated cells. Data represent mean ± SD. (n = 4 for B,C,G; n = 9 for E,F). * $P < 0.05$, analyzed by two-way ANOVA followed by Tukey's HSD test. Scale bars = 50 μm.

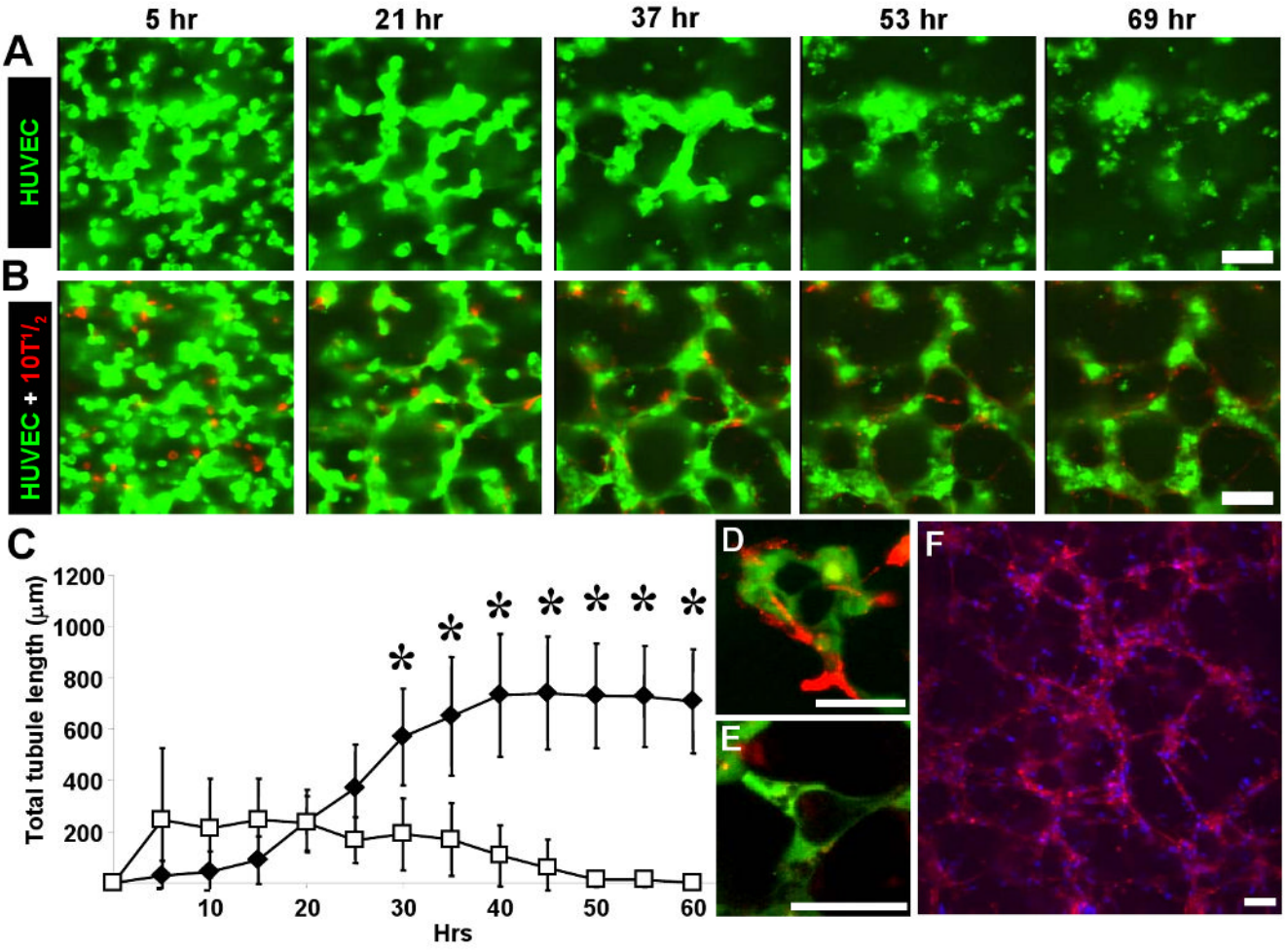

Figure 2. Time-lapse confocal videomicroscopy shows HUVECs and 10T1/2 undergoing tubule formation in hydrogels

Cellular interactions in hydrogels encapsulated with either A) HUVECs only or B) HUVECs and 10T1/2 cells were visualized over ~70 hrs with time-lapse confocal videomicroscopy. A) In HUVECs mono-culture conditions, tubule-like structures initially formed by cells failed to maintain their networks and quickly regressed after ~50 hrs of encapsulation in hydrogels. B) Tubule-like structures formed in co-culture conditions maintained their morphologies throughout the time-lapse experiments. C) The movies were analyzed quantitatively to plot tubule-length formed over time. Whereas the total tubule-length formed by HUVECs alone initially increased and sharply declined, there was a gradual increase and maintenance of the tubule-length in co-culture conditions. D) HUVECs with large vacuoles in their cell bodies and E) in the process of intercellular fusion of multiple vesicles to form large lumens were observed. 10T1/2 cells were recruited to the newly formed lumen or tubular structures. A,B,D,E) HUVECs and 10T1/2 cells were pre-stained with CellTracker Green and Red, respectively, prior to encapsulation into the hydrogels. F) HUVECs and 10T1/2 cells cultured for 28 days in hydrogels maintained the highly interconnected networks of tubules. F-actin and nuclei were stained by phalloidin-TRITC and DAPI, respectively. Data represent mean ± SD (n = 10-12). *P < 0.05, analyzed by two-way ANOVA followed by Tukey's HSD test compared to the HUVEC mono-culture groups. Scale bars = 50 μm.

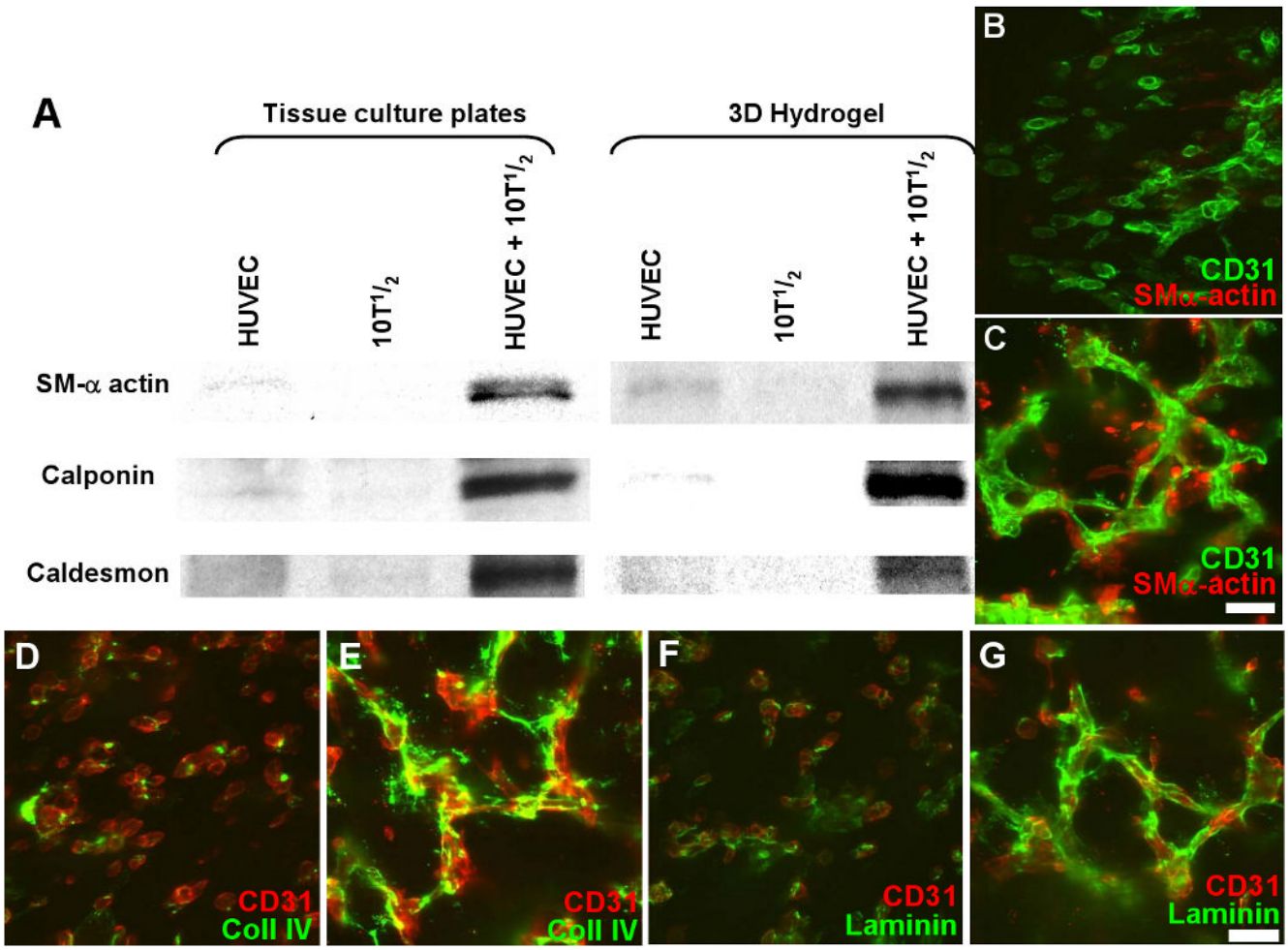

Figure 3. The tubule structures are stabilized by smooth muscle-like cells differentiated from 10T1/2 cells and by new deposition of collagen IV and laminin in hydrogels

A) HUVECs and 10T1/2 cells each cultured in mono-culture condition had minimal expression of SM-α actin, calponin, and caldesmon on tissue culture wells and in 3D network of hydrogels as shown by Western blotting. In contrast, in co-culture conditions, the expression levels of these SMC protein markers were dramatically up-regulated both on tissue culture wells and in the hydrogels by day 6. B) In hydrogels with HUVECs and 10T1/2 cells, there was minimal expression of SM-α actin on day 1, but C) by day 6, expression of SM-α actin was localized adjacent to CD31 staining specific for ECs, indicating that 10T1/2 cells up-regulated expression of the SMC marker protein. In the PEG hydrogels cultured with HUVECs and 10T1/2 cells for 1 day, there was minimal expression of D) collagen type IV or F) laminin; however, by day 6, the tubule-like structures were highly decorated with E) collagen type IV and G) laminin, indicating that the encapsulated cells are actively producing their own set of ECM proteins, thereby remodeling the synthetic matrices. B,C) Anti-CD31 immunostainings and anti-SM-α actin are shown in green and red, respectively. D-G) Anti-CD31 is shown in red, while anti-collagen type IV (D,E) and anti-laminin (F,G) are shown in green. Scale bars = 50 μm.

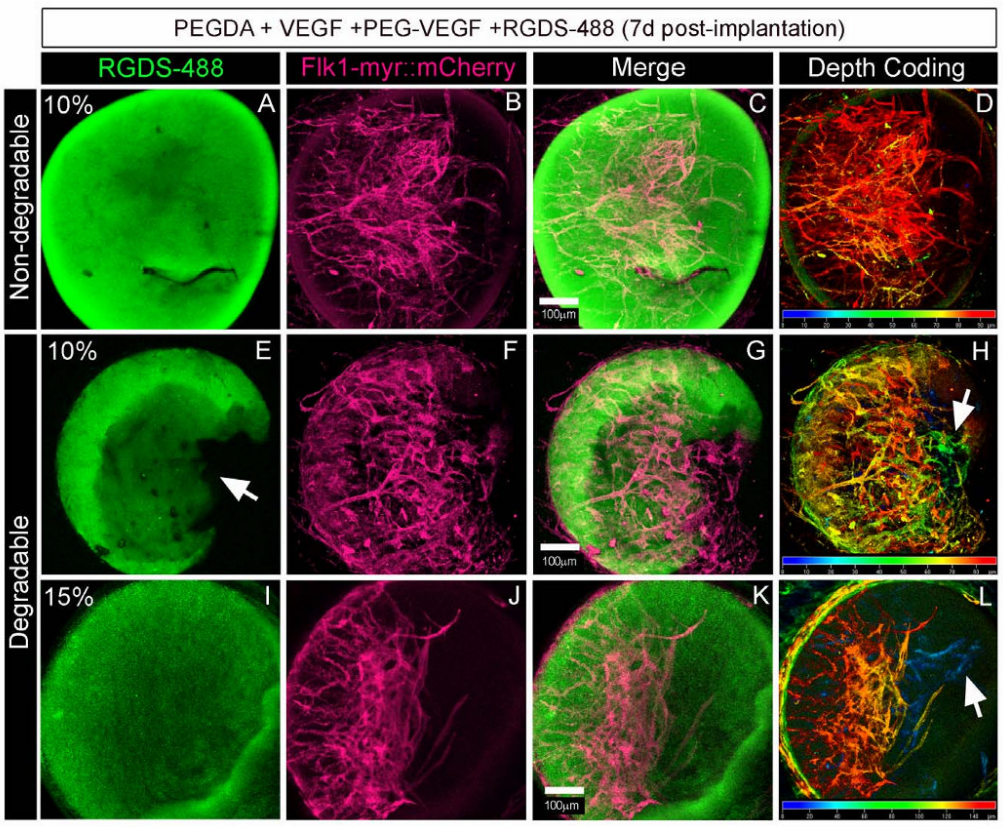

Figure 4. Proteolytically-degradable PEG hydrogels promote neovascularization in murine cornea

Hydrogels incorporated with soluble and immobilized form of VEGF via PEG linkage were implanted into cornea in *Flk1-myr::mCherry* transgenic mice. Newly formed blood vessels were visualized by confocal microscopy, and depth profiles of the vessels were generated to reveal their Z position with respect to the hydrogels. A-D) Non-degradable hydrogels releasing soluble VEGF supported angiogenesis adjacent to the hydrogels, but the depth decoding graph indicates lack of vessel penetration into the hydrogels. E-H) MMP-sensitive PEG hydrogels with 10% polymer weight promoted robust neovascularization adjacent to the hydrogels and extensive infiltration of host vasculature into the hydrogels. The arrow in E) indicates a portion hydrogel undergoing active degradation, and the arrow in H) points to regions within hydrogels with vessel infiltration. I-L) MMP-sensitive PEG hydrogels with 15% polymer weight had blood vessel growth on surface of hydrogels as pointed by the arrow in L), but the hydrogels remained mostly intact (I) without any significant vessel infiltration into the core. Scale bars = 100 μm in A-L).

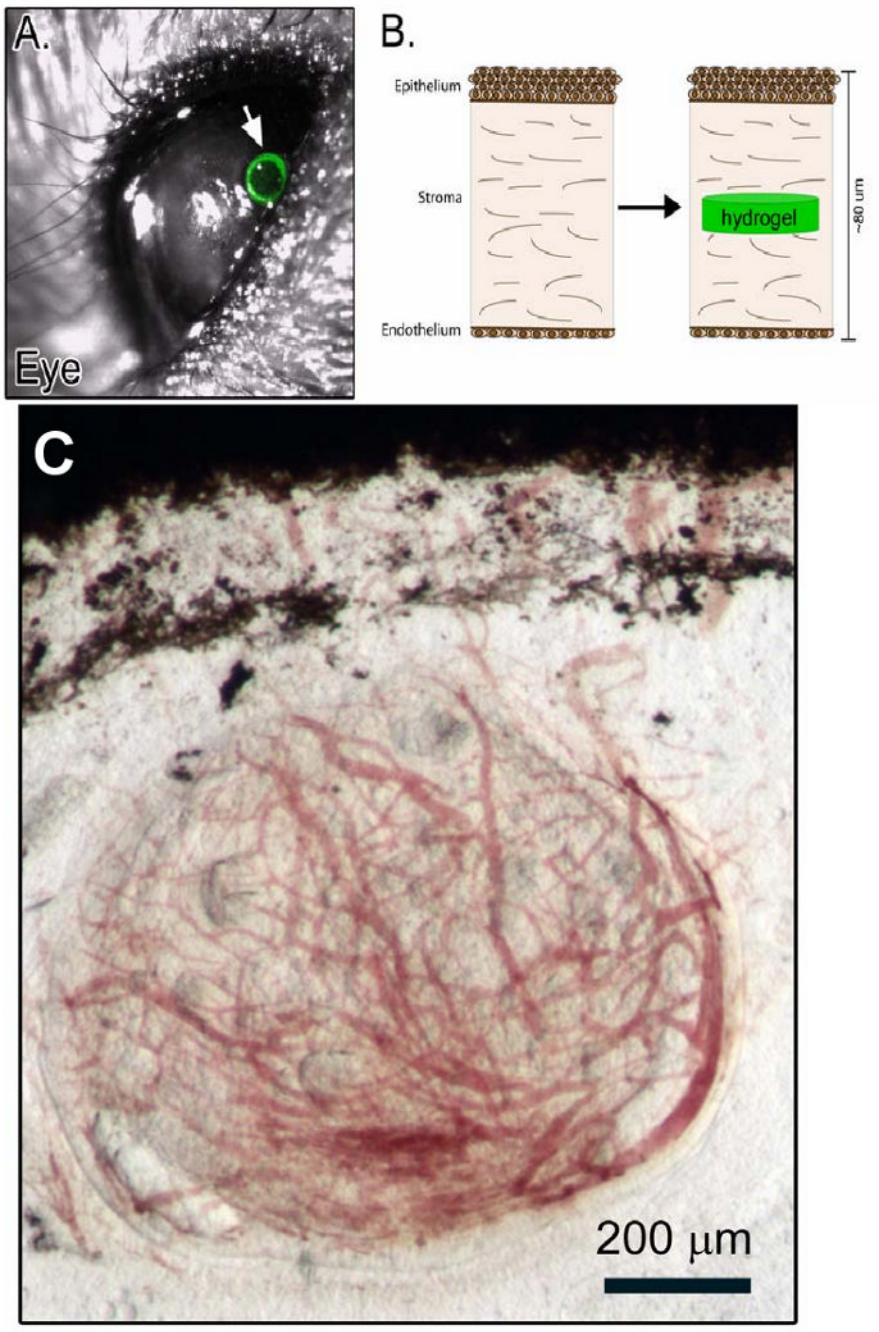

Figure 5. Newly formed blood vessels in hydrogels are functional

A,B) Small incision was made in cornea and photopolymerized hydrogels were implanted into the micropocket. C). Blood vessels formed in the hydrogels were perfused with Dextran-Texas red (70KDa MW) injected intravenously into mice.